

Earth's Future



RESEARCH ARTICLE

10.1029/2023EF003779

Key Points:

- We determine the changes of West African Summer Monsoon precipitation using stratospheric aerosol geoengineering injections climate models
- Increase of precipitation is presented under global warming while its decrease is obtained with stratospheric aerosol geoengineering models
- These changes of West African Summer Monsoon precipitation are mainly driven by the dynamic processes

Supporting Information:

Supporting Information may be found in the online version of this article.

Correspondence to:

F. Bonou,
fredericbonou@yahoo.fr

Citation:

Bonou, F., Da-Allada, C. Y., Baloitcha, E., Alamou, E., Biao, E. I., Zandagba, J., et al. (2023). Stratospheric sulfate aerosols impacts on West African monsoon precipitation using GeoMIP models. *Earth's Future*, 11, e2023EF003779. <https://doi.org/10.1029/2023EF003779>

Received 23 MAY 2023
Accepted 27 OCT 2023





Author Contributions:

Data curation: Frédéric Bonou, Casimir Yelognisse Da-Allada
Formal analysis: Frédéric Bonou, Yves Pomalegni, Peter James Irvine
Investigation: Frédéric Bonou, Casimir Yelognisse Da-Allada, Yves Pomalegni
Methodology: Frédéric Bonou, Casimir Yelognisse Da-Allada
Supervision: Peter James Irvine
Validation: Frédéric Bonou, Casimir Yelognisse Da-Allada

© 2023 The Authors.

This is an open access article under the terms of the [Creative Commons Attribution-NonCommercial License](https://creativecommons.org/licenses/by-nc/4.0/), which permits use, distribution and reproduction in any medium, provided the original work is properly cited and is not used for commercial purposes.

Stratospheric Sulfate Aerosols Impacts on West African Monsoon Precipitation Using GeoMIP Models

Frédéric Bonou^{1,2,3} , Casimir Yelognisse Da-Allada^{1,4} , Ezinvi Baloitcha¹, Eric Alamou⁴, Eliezer Iboukoun Biao⁴ , Josué Zandagba⁴, Ezéchiél Obada⁴, Yves Pomalegni¹, Peter James Irvine⁵, and Simone Tilmes⁶ 

¹International Chair in Mathematical Physics and Applications (ICMPA—UNESCO CHAIR), University of Abomey-Calavi, Abomey, Benin, ²Laboratory of Physics and Applications (LPA), National University of Sciences, Technology, Engineering and Mathematics (UNSTIM), Natitingou, Benin, ³Laboratory of Marine and Coastal Hydrology, Institute of Fisheries and Oceanographic Research of Benin (IRHOB), Cotonou, Benin, ⁴Laboratory of Geosciences, Environment and Applications, National University of Sciences, Technology, Engineering and Mathematics, UNSTIM/Abomey, Abomey, Benin, ⁵University College London, London, UK, ⁶National Center for Atmospheric Research, Boulder, CO, USA

Abstract Stratospheric Aerosol Geoengineering (SAG) is proposed to offset global warming; however, the use of this approach can have an impact on the hydrological cycle. We used simulations from Coupled Model Intercomparison Project (CMIP5) and Geoengineering Model Intercomparison Project (G3 simulation) to analyze the impacts of SAG on precipitation (P) and to determine its responsible causes in West Africa and Sahel region. CMIP5 historical data were first validated, the results obtained are consistent with observational data. Under the Representative Concentration Pathway scenario RCP4.5, a slight increase is found in the West Africa Region relative to present-day climate. The dynamic processes especially, the monsoon shifts are responsible for this precipitation change. Under RCP4.5, during the monsoon period, reductions in P are 0.86%, 0.80% relative to the present-day climate in the Northern and Southern Sahel, respectively, while precipitation is increased by 1.04% in the West African Region. Under SAG, we find a 3.71% decrease of precipitation in the West African Region while the precipitation decrease is 17.4% and 8.47% respectively in the North Sahel and South Sahel. This decrease in monsoon precipitation is mainly explained by changes in dynamics, which lead to weakened monsoon circulation and a shift in the distribution of monsoon precipitation. This result suggests that SAG deployment to balance all warming can be harmful to rainfall in WAR if the amount of SO_2 to be injected into this tropical area is not taken into consideration.

Plain Language Summary Stratospheric Aerosol Geoengineering (SAG) deployment has been proposed to reduce temperature increase in the context of global warming but its impacts on the hydrological cycle and the underlying causes need to be evaluated on the regional scale. While some effects of Stratospheric Aerosol Geoengineering on the water cycle are uncertain, various studies suggest that there could be considerable changes in regional rainfall. Climate simulations (Coupled Model Intercomparison Project: CMIP5 and Geoengineering Model Intercomparison Project: GeoMIP) are used in this work to quantify the impacts on the monsoon rainfall in West Africa. We determine the changes in precipitation and the mechanisms responsible for these changes in West Africa during summer using Stratospheric Aerosol Geoengineering. Under global warming, while a slight decrease of precipitation is noted in the Sahel region, a significant decrease in rainfall is obtained over the West Africa region and the Sahel region under SAG. The main processes responsible for the changes of precipitation under SAG are determined based on the decomposition approach. Results show that changes in precipitation are largely related to changes in dynamic processes (monsoon circulation).

1. Introduction

The West African Summer Monsoon (WASM) is a system of Earth's climate that involves interconnections between the atmosphere, the biosphere, and the hydrosphere over many time scales during the boreal summer (e.g., Nicholson & Grist, 2003; Redelsperger et al., 2006). It is part of the global monsoon system, which regulates atmospheric humidity and heat budgets in low latitudes. It is the major source of water for agriculture in West Africa (Froidurot & Diedhiou, 2017) and also the principal determinant of agricultural production in densely populated areas where the economy is dependent on subsistence farming and the agricultural system is relying on precipitation. The WASM precipitation is characterized by moisture fluxes derivation from different

Visualization: Frédéric Bonou, Peter James Irvine

Writing – original draft: Frédéric Bonou

Writing – review & editing: Frédéric Bonou, Casimir Yelognisse Da-Allada, Eliezer Iboukoun Biao, Yves Pomalegni, Peter James Irvine, Simone Tilmes

sources comprising the soil moisture and the atmospheric moisture flux convergence (Lélé et al., 2015; Mera et al., 2014). Some previous works investigated the atmospheric moisture over the WASM. Pomposi et al. (2015) noticed that changes in moisture flux convergence, as well as the circulation process within the monsoon region and along the monsoon border, are associated with the precipitations changes within the Intertropical Convergence Zone (ITCZ). In the WASM zone, the role of continental surfaces is widely recognized due to the close relationship associated with soil moisture and precipitation (Xue & Shukla, 1993).

The WASM variability poses a constraint to the water resources, vegetation, and food security and its long-term state over periods of a few years to several decades (Abiodun et al., 2008; Janicot, 1992; Lamb, 1982; Nicholson, 2013; Okoro et al., 2018; Sanogo et al., 2015). In West Africa, more than 80% of the annual rainfall occurs during June–September when the intertropical front is in northward position. WASM region frequently experiences droughts, which cause water deficiencies and disrupt the agriculture sector and affect food and income for the majority of rural households. The impacts of these droughts and the controversy concerning their causes has prompted climatologists to offer a variety of hypotheses including changes in the ITCZ latitude position, tropical Atlantic Sea surface temperature anomalies, and energy balance changes (Chou et al., 2004; Schneider et al., 2014).

Understanding rainfall variability and its impacts at different time scales (past, present, and future) requires future projection models in the context of global warming and climate geoengineering. Stratospheric Aerosol Geoengineering (SAG) is one of the geoengineering methods (Lenton & Vaughan, 2009) that could lead to a reduction in global warming. The method could be relatively low cost, especially in comparison with the cost of mitigation, potentially making this idea attractive to policymakers and stakeholders (Robock et al., 2009). Stratospheric Geoengineering Aerosol injection could have causal consequences on the hydrological cycle, and thus, the region of monsoon precipitation could be impacted (Kravitz et al., 2013; Robock et al., 2009; Tilmes et al., 2013a, 2013b). Most of the previous studies have been focused on the determination of geoengineering impacts on precipitation at the global scale and have reported the reduction of the hydrological cycle with SAG injection (Govindasamy & Caldeira, 2000; Kravitz et al., 2013; Tilmes et al., 2013a, 2013b). Although some research works have investigated the main mechanisms of the impacts of SAG on precipitation in West Africa (Da-Allada et al., 2020), there is still a need to deepen the knowledge of precipitation changes in West Africa of the different existing models and SAG scenarios.

Increasing of WASM patterns, induced by anthropogenic greenhouse gas and aerosol forcing, may have led to a significant increase in Sahel precipitation since the 1980s (Dong & Sutton, 2015). Under RCP8.5, approximately 80% of CMIP5 models agree on a modest drying rate of around 20% over the westernmost Sahel (15°W–5°W), whereas approximately 75% of models agree on an increase in precipitation between 0°E and 30°E over the Sahel, with a wide amplitude distribution (Roehrig et al., 2013). The projected reinforcement of WASM is related to a robust expansion of warming over the Sahel by around 10%–50% over the global mean (Roehrig et al., 2013). Previous works done by Da-Allada et al. (2020), Odoulami et al. (2020), and Pinto et al. (2020) showed that the application of SAG would affect temperature and precipitation over sub-Saharan Africa using GLENS simulations. They found that the use of SAG would lead to a reduction in temperature and extreme precipitation. It has been shown that the use of SAG in the northern hemisphere only could affect the hydrological cycle in the Sahel, while the SAG injection in only the Southern Hemisphere may increase significantly the Sahel vegetation productivity (Haywood et al., 2013). These authors showed that the deployment of SAG in only one hemisphere may affect the position of the Inter tropical Convergence Zone (ITCZ). Interpreting variations in global mean precipitation, Kravitz et al. (2013) described the changes in the surface and atmospheric energy budgets using GeoMIP simulations (Kravitz et al., 2011) reported that precipitation changes could be attributed to a decrease in the mean flux of evaporative moisture and increased moisture convergence, particularly over land regions. Furthermore, using GeoMIP simulations, Kravitz et al. (2013) and Tilmes et al. (2013a, 2013b) reported the large decline in land evaporation in most regions associated with the global decline in precipitation, this is not the case in the summer monsoon rainfall regions of West Africa, whereas summer monsoon rainfall is influenced by both regional and large-scale processes. Consequently, the mechanisms responsible for changes in WASM still need more investigation. Changes in tropical precipitation can be demonstrated through the decomposition into the contributions of thermodynamic and dynamic processes (e.g., Weller et al., 2019), and the decomposition methodology of Chadwick et al. (2013, 2016) can be used to identify the related contribution of these two terms (Chadwick et al., 2016; Kent et al., 2015; Lazenby et al., 2018; Monerie et al., 2019). Using this method, changes in tropical precipitation, under climate change, have been largely associated with changes in the dynamic

component indicating changes in the position of ITCZ (Chadwick et al., 2016; Kent et al., 2015). Due to the great importance of WASM on agriculture productivity, its magnitudes and its change under geoengineering need to be investigated regionally, and climate modeling should be a helpful way in this analysis. The utilization of climate geoengineering is anticipated to offset the warming caused by rising greenhouse gas levels by simultaneously reducing solar absorption, linked with a reduction in precipitation (Crutzen, 2006). Geoengineering atmosphere models basing on sulfate aerosols also show changes in stratospheric dynamics and chemistry caused by SAG (Heckendorn et al., 2009; Tilmes et al., 2009).

In the current study, the changes under SAG on WASM have been determined using GeoMIP (G3/G4) and Coupled Model Intercomparison Project CMIP5 (Historical, RCP4.5) simulations after validation with CMAP and GPCP observations. These impacts of SAG are determined in the context of global warming and climate geoengineering with their main causes to explain the changes. The rest of the manuscript is organized as follows, Methods and data, the section in which present the set of data and methods used in this study. Results describe the validation of historical simulation in comparison to CMAP and GPCP observations. The impacts of SAG on WSAM precipitation are presented in this same section under different simulations. The potential mechanisms explaining the changes in monsoon precipitation have been determined based on IPSL-CM5A-LR due to availability of specific humidity with higher vertical resolution. The next section is dedicated to the results Discussions. Finally, the conclusion presents a summary of the results obtained in this paper.

2. Data and Methodology

2.1. Observations and Models Data

This study is conducted in West Africa (Figure 1), focusing on three subregions within West Africa considered, Northern Sahel (NSA) and Southern Sahel (SSA), and Western Africa Region (WAR). Eleven models of CMIP5 with two experiments (Historical and RCP4.5 simulations) are analyzed in this paper; these models are listed in Table 1. These historical CMIP5 models are extracted from the global data for West Africa during the monsoon period (Figure 1). Two observed precipitation data sets (Global Precipitation Climatology Precipitation: GPCP and CPC Merged Analysis Precipitation: CMAP) gridded at a horizontal resolution of $2.5^\circ \times 2.5^\circ$ of horizontal resolution have been used for the comparison with model data.

The historical simulations comprise model data which have been extracted for West Africa covering the period from 1986 to 2005 (20 years). In addition, the available GeoMIP (G3/G4) data have been also used in this study with associated RCP4.5 simulations of CMIP5 models. For each model, daily or monthly data from (historical experiments of CMIP5 models) are jointly analyzed with RCP4.5. The CMIP5 models have different simulations; their Historical simulations represent the recent past data (Sheffield et al., 2013). The CMIP5 Historical simulations include all forcing have been applied to the models, including anthropogenic greenhouse gas concentrations. The historical simulation began from multicentury preindustrial control runs and is configured to account for atmospheric composition evolution (anthropogenic and natural sources). The RCP4.5 is a Representative Concentration Pathway (RCP 4.5) with a scenario that provides stabilization to radiation forcing at 4.5 W.m^{-2} in the future projection spanning from 2006 to 2100 without ever exceeding that value. This simulation incorporates historical emissions and land cover information. G3 is an SAG simulation based on the RCP4.5 scenario, with deployment starting in 2020 and gradually ramping-up the amount of SO_2 or sulfate aerosol injected, to keep global average temperature nearly constant at 2020 levels (Kravitz et al., 2011). G4 is similar except that starting from 2020 it applies a constant injection of SO_2 at a rate of 5 Tg SO_2 per year (Bürger et al., 2015; Clarke et al., 2021; Kravitz et al., 2011). Both G3 and G4 inject SO_2 into the equatorial stratosphere at the altitude range of 16–25 km at 0° longitude on the equator. The main variables extracted from each simulation in this work include precipitation (P), wind velocity (V) and specific humidity (q).

2.2. Methodology

The monthly mean of historical simulations is used for the model validation with observations data from 1986 to 2005 for the monsoon period during boreal summer starting from July to October. The changes in rainfall have been calculated through the difference between all the existing ensemble members of RCP4.5 over 2050–2069 and the baseline (present-day climate: 2010–2029) under global warming. Under SAG, changes of precipitation have been quantified through the difference between the only ensemble member of G3 (2050–2069) and baseline (Table 1). We selected this future period (2050–2069) as the distribution of SO_2 injection rates converges around

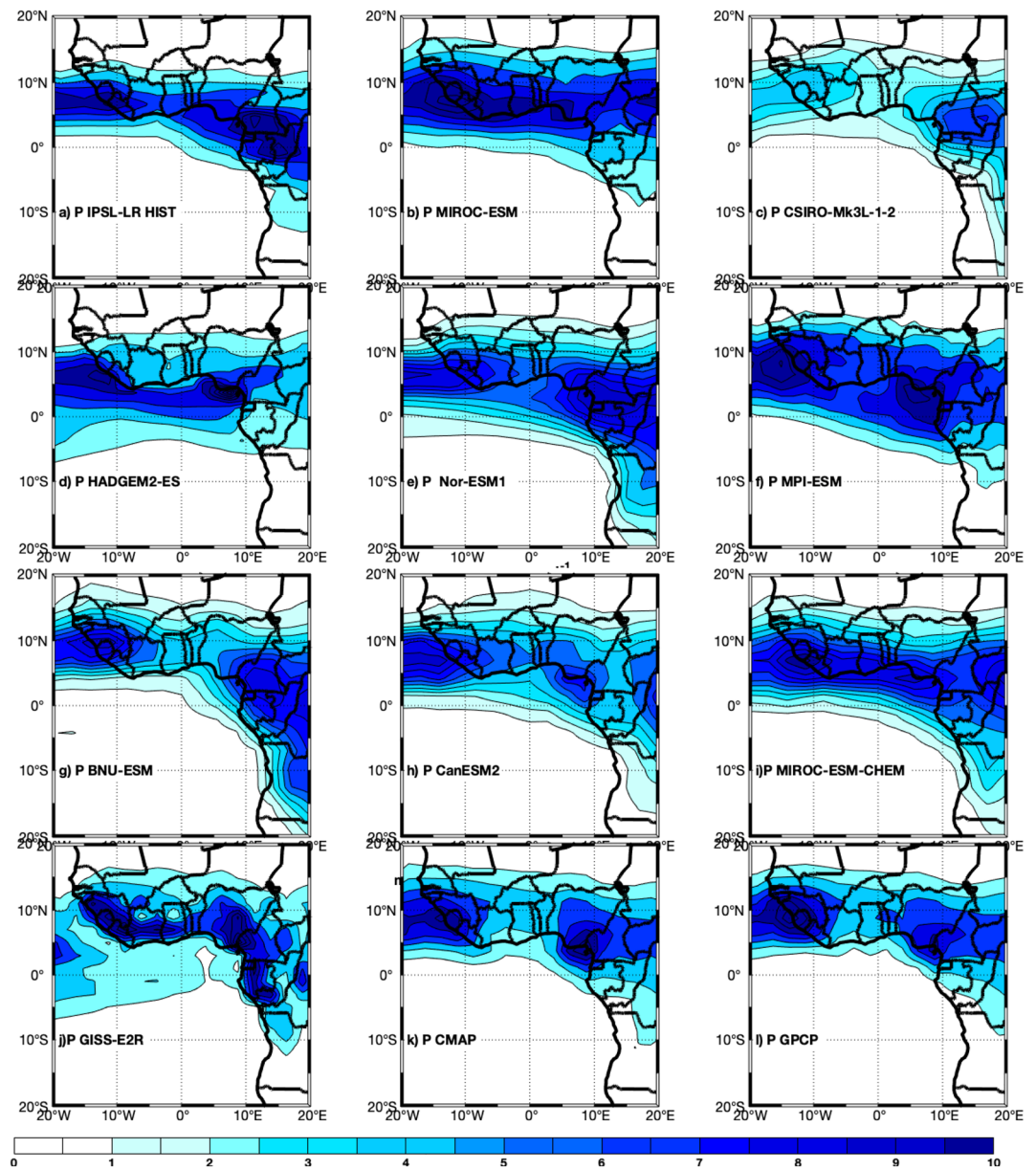


Figure 1. Spatial distributions of monthly precipitation (mm day⁻¹) averaged over 1986–2005 between July and October in West Africa from (a) to (j) from Historical CMIP5 simulations.

2050 (MacMartin et al., 2019). The baseline period is 20 years (2010–2029) period, which is considered as the period more suitable for present-day climate. The statistical significance of the rainfall changes is determined using a two-tailed Student's *t*-test and the standard error is used to provide an estimate of the error in the rainfall changes.

Precipitation change (ΔP) has been decomposed into dynamical (ΔP_{dyn}), thermodynamical (ΔP_{therm}) and non-linear cross components (ΔP_{cross}) according to Chadwick et al. (2013) to access the causes of precipitation changes in West Africa. In reality, this method assumes that the precipitation is dominated by convection in tropical regions (Chadwick et al., 2016; Monerie et al., 2019). The precipitation, P , is considered as $P = M^*q$, where M^* is defined as a proxy for convective mass flux from the boundary layer to the free troposphere (Held & Soden, 2006; Kent et al., 2015; Lazenby et al., 2018), $M^* = P/q$, and q is near surface specific humidity, then, the change in rainfall, then, ΔP is decomposed as:

$$\Delta P = M^* \Delta q + q \Delta M^* + \Delta q \Delta M^* \quad (1)$$

Table 1

List of Models Used in This Work (11 RCP4.5, 10 Historical, 9 G4, and 6 G3) Simulations (More Detail Can Be Found in Table S1 of the Supporting Information S1)

Models	G3 (members)	G4 (members)	Historical (members)	RCP4.5 (members)	Reference
MPI-ESM-LR	3	Not available	3	3	Bentsen et al. (2013)
NorESM1-M	2	1	3	1	Bentsen et al. (2013)
BNU-ESM	1	1	1	1	Versteine et al. (2010)
CanESM2	Not available	3	4	10	Chylek et al. (2011)
CSIRO-MK3L-1-2	Not available	3	4	3	Parth et al. (2016)
GISS-E2-R	3	3	9	3	Schmidt et al. (2014)
HadGEM-ES	3	3	4	4	Collins et al. (2011)
IPSL-CM5A-LR	1	Not available	6	5	Dufresne et al. (2013)
MIROC-ESM	Not available	1	3	3	Watanabe et al. (2011)
MIROC-ESM-CHEM	Not available	9	1	9	Watanabe et al. (2011)
GEOSCCM	Not available	3	Not available	3	Duncan et al. (2007)

Note. G3, G4, and RCP4.5 simulations: 2050–2069. Baseline simulations (RCP4.5): 2010–2029. CMIP5 historical simulations: 1986–2005.

$$= \Delta P_{\text{therm}} + \Delta P_{\text{dyn}} + \Delta P_{\text{cross}}$$

where ΔP_{therm} is the thermodynamic change due to the specific humidity changes (q), ΔP_{dyn} represents the dynamic change from circulation changes (M^*), and ΔP_{cross} is the term due to the changes in both specific humidity and circulation. Further decomposition of ΔP_{dyn} allows us to document changes due to shifts in the pattern of tropical circulation (ΔP_{shift}) or tropical weakening circulation (ΔP_{weak}) which represents the mean tropical circulation

$$\Delta P_{\text{dyn}} = \Delta P_{\text{weak}} + \Delta P_{\text{shift}} \quad (2)$$

$$\Delta P_{\text{weak}} = q \Delta M^*_{\text{weak}} \quad (3)$$

$$\Delta P_{\text{shift}} = q \Delta M^*_{\text{shift}} \quad (4)$$

$$\Delta M^*_{\text{weak}} = -\alpha M^* \quad (5)$$

where ΔM^*_{weak} with $\alpha = (\text{tropical mean } \Delta M^*) / \text{tropical mean } M^*$ is the change in the strength of the mean tropical circulation. Note that although ΔM^* is a scalar, ΔP_{weak} is provided for each grid point by multiplying by the reference moisture field. $\Delta M^*_{\text{shift}}$ is calculated by removing ΔM^*_{weak} from ΔM^* (i.e., $\Delta M^*_{\text{shift}} = \Delta M^* - \Delta M^*_{\text{weak}}$).

The efficacy of precipitation change has been computed according to Cheng et al. (2019) using the following equation:

$$\text{Efficacy} = \frac{\Delta P(G3 - RCP4.5)}{\Delta P(RCP4.5 - \text{Baseline})}$$

$\Delta P(G3 - RCP4.5)$ represents the difference between G3 and RCP4.5 precipitation and $\Delta P(RCP4.5 - \text{Baseline})$ represents the difference between the RCP4.5 and baseline precipitation. This ratio helps to provide the information on the effectiveness of the application of SAG injection in a specific region and can be expressed in percentage.

3. Results and Discussion

3.1. Validation of Historical Simulation

Historical simulations of Precipitation from CMIP5 models have been compared with GPCP and CMAP observations for the same period (Figure 1). Most of the CMIP5 simulations used in this work are relatively in good agreement with the observations (CMAP, GPCP), the maxima of WASM mostly oscillated between the equator and 10°N latitude during African monsoon period, although some differences in the position of the maxima of precipitation appear in the extension of high precipitation extending southward varies from one simulation to

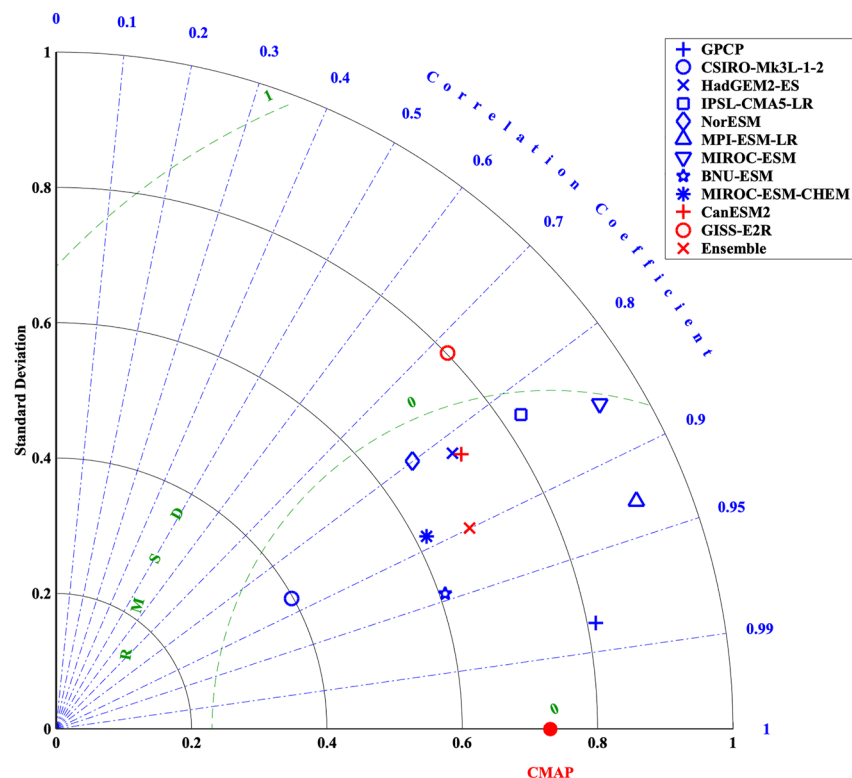


Figure 2. Taylor diagrams showing monthly precipitation averaged over 1986–2005 between July and October in West Africa. The red dot is the CMAP precipitation considered as the observations data.

another (Figure 1). The CSIRO simulation exhibits a higher underestimation of precipitation. The zone of maximum precipitation is well represented. In general, all models agree with the distribution of maximum precipitation distribution, from the ocean to inland regions with an intensification of precipitation during the monsoonal period, with the values reaching approximately 10 mm d^{-1} .

The performances of each Historical CMIP5 precipitation in West Africa are statistically summarized using the Taylor diagram (Figure 2) to identify the models that closely match observation data. This diagram provides a concise statistical evaluation of the degree of pattern correspondence between the models and observations, considering Pearson's correlation (Cor), root-mean-square error (RMSE), and the ratio of their variances (STD). All simulations reproduce the observed CMAP monsoonal precipitation relatively well, but also match GPCP observations in West Africa (Figure 2). The root mean square deviation values to CMAP precipitation in all historical simulations are less than $\sim 2 \text{ mm day}^{-1}$, except for GISS-E2R. This tool indicates the position of the correlation coefficient with a 95% of significance level. These values of correlations coefficient are situated between 0.8 and 0.9, except for the GISS-E2R, which, has a correlation value of 0.71.

The analysis of precipitation biases is described by estimating of the difference between each model and the CMAP observations. Dry biases (approximately 5 mm day^{-1}) have been observed over West Africa and the Sahel region from one model to another. IPSL-CM5A-LR, MIROC-ESM-CHEM, HadGEM2-ES, MPI-ESM, Nor-ESM1, BNU-ESM, and CanESM2 all show an underestimation of precipitation over the Sahel region, while a modest overestimation is observed over West Africa and coastal regions (Figure 3). CSIRO-Mk3L-1-2 mostly exhibits a high underestimation compared to the observation over the West Africa and the Sahel region. The ensemble simulations of CMIP5 models show that their historical simulations tend to have lower rainfall in the over Sahel region, while higher precipitation is distributed over some coastal countries and the southern part of West Africa.

3.2. Precipitation Changes Under Global Warming (RCP4.5-Baseline)

Under global warming, changes in precipitation have been estimated by calculating the difference between each RCP4.5 model and its baseline simulation. Different patterns of precipitation changes have been observed over

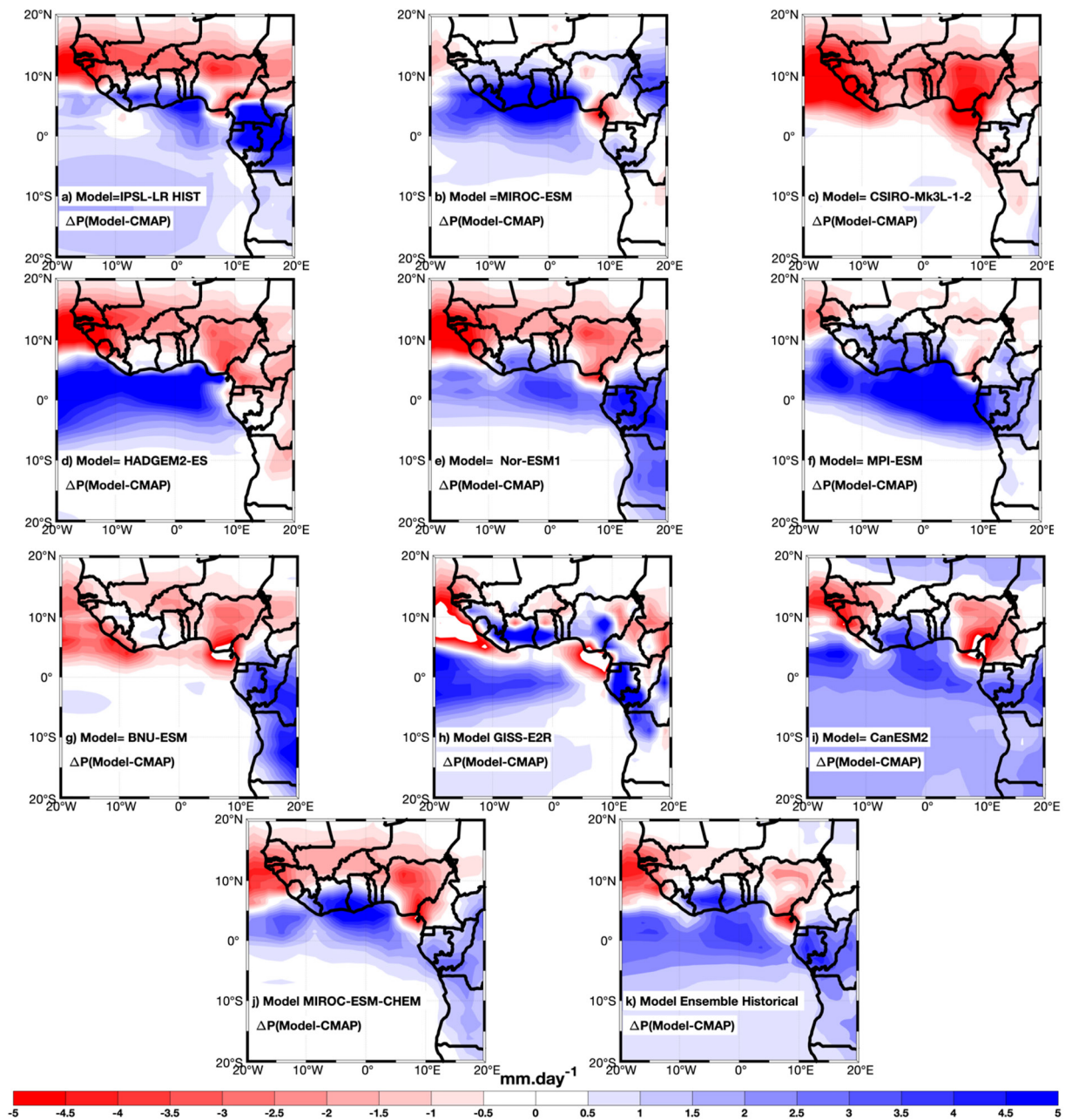


Figure 3. Difference of precipitation between Models and CMAP observations over 1986–2005 between July and October in West Africa.

West Africa and the Sahel region (Figure 4). The ensemble simulation mostly exhibits an increase in precipitation over West Africa and Sahel region. The results vary from one model to another. Negatives changes are observed over West Africa and the Sahel region in MPI-ESM, BNU-ESM, Nor-ESM1, and MIROC group models. This pattern of precipitation with these simulations is opposite to that of the rest of RCP4.5 simulations and the ensemble simulations.

3.3. Precipitation Changes Under Stratospheric Aerosol Injection on Monsoon Precipitation

The precipitation changes under different G3 simulations have been estimated by determining the difference between G3 and baseline simulations (RCP4.5, from 2010 to 2029). Most of the models show a decrease in precipitation over the West Africa region and Sahel region (Figure 5) except for GISS-E2R and HadGEM-ES.

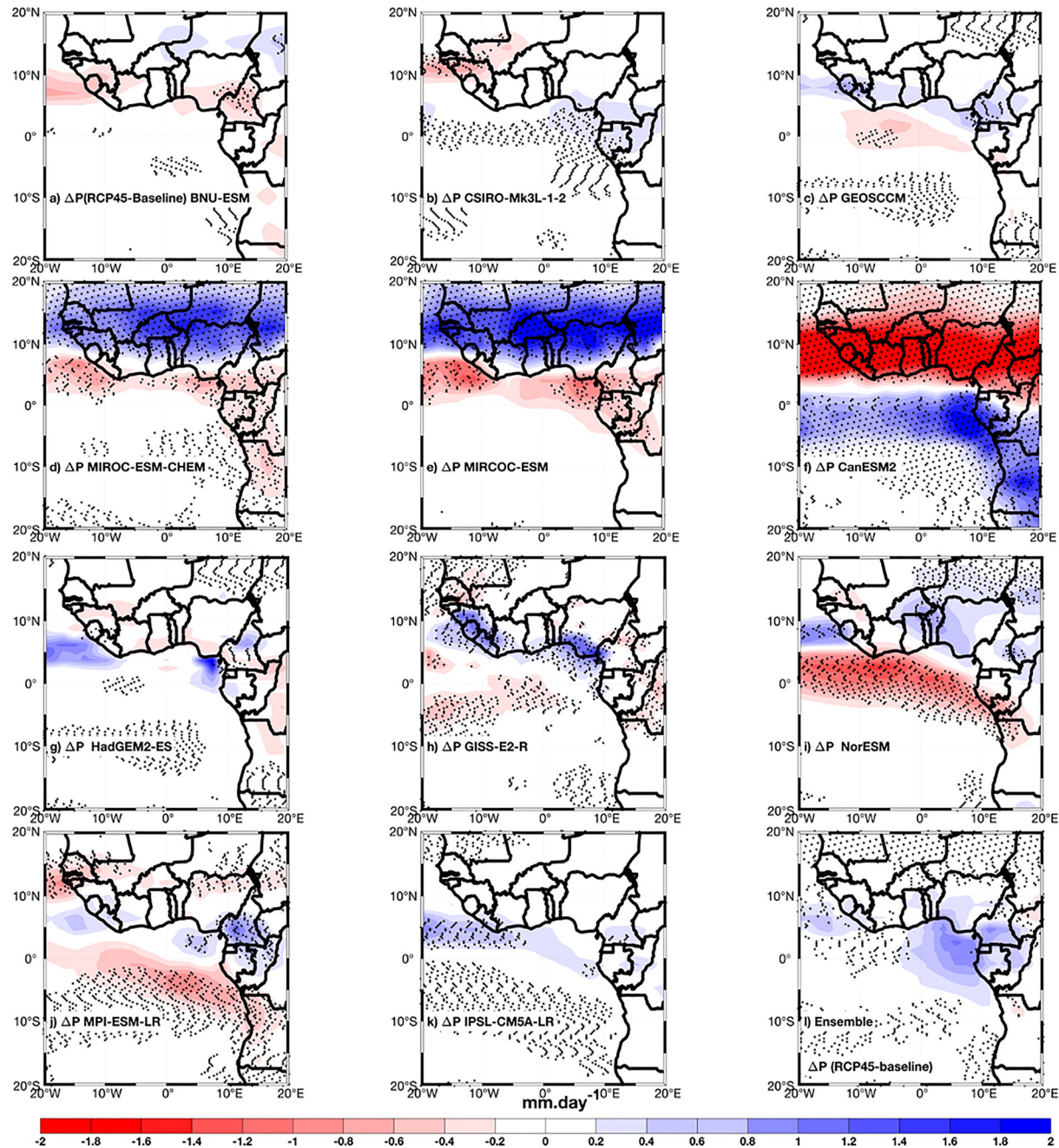


Figure 4. Changes of precipitation between Models and baseline (RCP4.5-baseline) simulations during the monsoon period (July–October). The black cross represents the areas of significance (*t*-test of student, 95% of significance).

The ensemble of G3 experiments mostly shows a decrease in precipitation over Sahel region and West Africa region except some coastal countries (Figure S3 in Supporting Information S1). This increase is essentially due to the positive changes in GISS-E2R and HadGEM-ES along coastal region.

G4 simulations are the second scenarios analyzed in this study as one of the SAG scenarios. The changes of precipitations are also estimated by retrieving its associated baseline (Figure 6). The models, BNU-ESM, CSIRO-Mk3L-1-2 and GEOSCCM show an overall decrease (approximately 1 mm day^{-1}) in precipitation over West Africa and the Sahel regions. However, MIROC-ESM, MIROC-ESM-CHEM present an increase in precipitation over Sahel region. This set of models affects the ensemble simulation, which presents a higher increase in

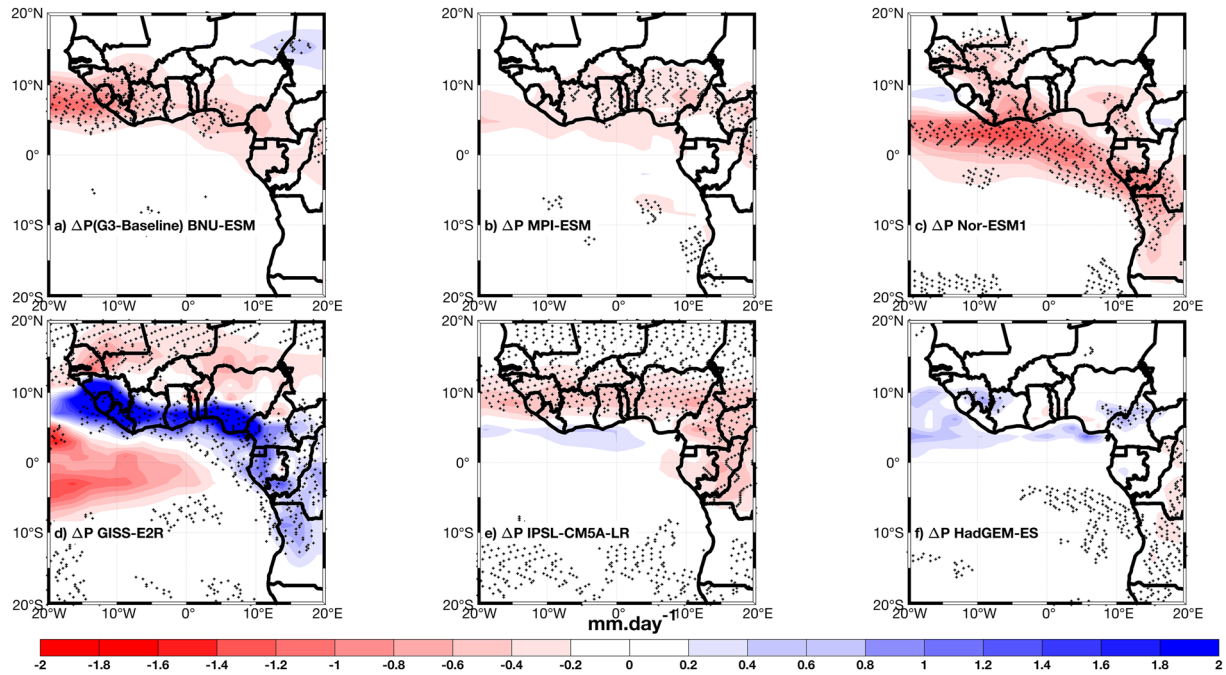


Figure 5. Precipitation changes between Models and baseline (G3-baseline) simulations during the monsoon period, July–October. The baseline or reference period is from 2010 to 2029 and the future period for G3 is from 2050 to 2069 for different models. The cross points represent the zone of significance with 95% of significance.

precipitation over West Africa and in G4 simulation. Most of G4 simulations show an increase in precipitation (Figure 6). Consequently, the ensemble simulations present also the increase of precipitation.

3.4. Mechanisms Explaining Precipitation Changes in West Africa

The IPSL-CM5A-LR model is used in this work to analyze the main mechanism driving precipitation changes under SAG and global warming. The choice of this models is based on the availability of specific humidity data at pressure levels near 955 hPa in IPSL-CM5A-LR. In this work, RCP4.5 simulations have been chosen as G3 simulations, derived directly from RCP4.5. Under RCP4.5 conditions of global warming, the change in monsoonal precipitation is determined by computing the difference in precipitation between two different periods (RCP4.5: 2050–2069) relative to the baseline (RCP4.5: 2010–2029). An increase in summer monsoon precipitation is most notable toward the oceanic zone adjacent to the West Africa region (Figure 7a). In the region of study, the changes in precipitation are statistically significant where the dot points are located in Figure 7. However, the main processes responsible for the precipitation changes (ΔP) under RCP4.5 are mainly due to monsoon precipitation shifts in the distribution (ΔP_{shift}). Additionally, we also notice a contribution of thermodynamic changes offset by the high impact of ΔP_{weak} . The dynamic process (Figures 7b–7d) is the major mechanism controlling the precipitation changes. The ΔP_{cross} contribution is low regarding precipitation changes (Figure 7c). The increase in ΔP_{therm} distribution appears from the equator toward the northern part; this pattern also contributes slightly to the change in precipitation under global warming (Figures 7b and 7g). This pattern of ΔP_{therm} is explained by the increase in specific humidity (Figures 7a and 7b). ΔP_{dyn} distribution shows mostly a decrease between 5° and 10°N. A slight decrease (approximately -0.1 mm day^{-1}) appears over the Sahel region (both North and South region) under RCP4.5 simulation.

ΔP_{dyn} term has been decomposed according to Equation 2 by dissociating this term into a component associated with the local dynamic feedback responsible for the shift in monsoon precipitation distribution (ΔP_{shift}). The spatial distribution of ΔP_{weak} presents the contrast pattern with ΔP_{therm} (Figures 7b and 7e). The amplitude of ΔP_{therm} is slightly greater than that of ΔP_{weak} , as the sum of ΔP_{therm} (positive) and ΔP_{weak} (negative) present a slightly positive variation (Figure 7g). The distribution of ΔP_{shift} has a similar pattern to that of precipitation (Figures 7a and 7f), therefore ΔP_{shift} component of ΔP_{dyn} is largely responsible for the changes in ΔP . The change of precipitation under RCP4.5 based on the decomposition method is similar to the change of the sum of

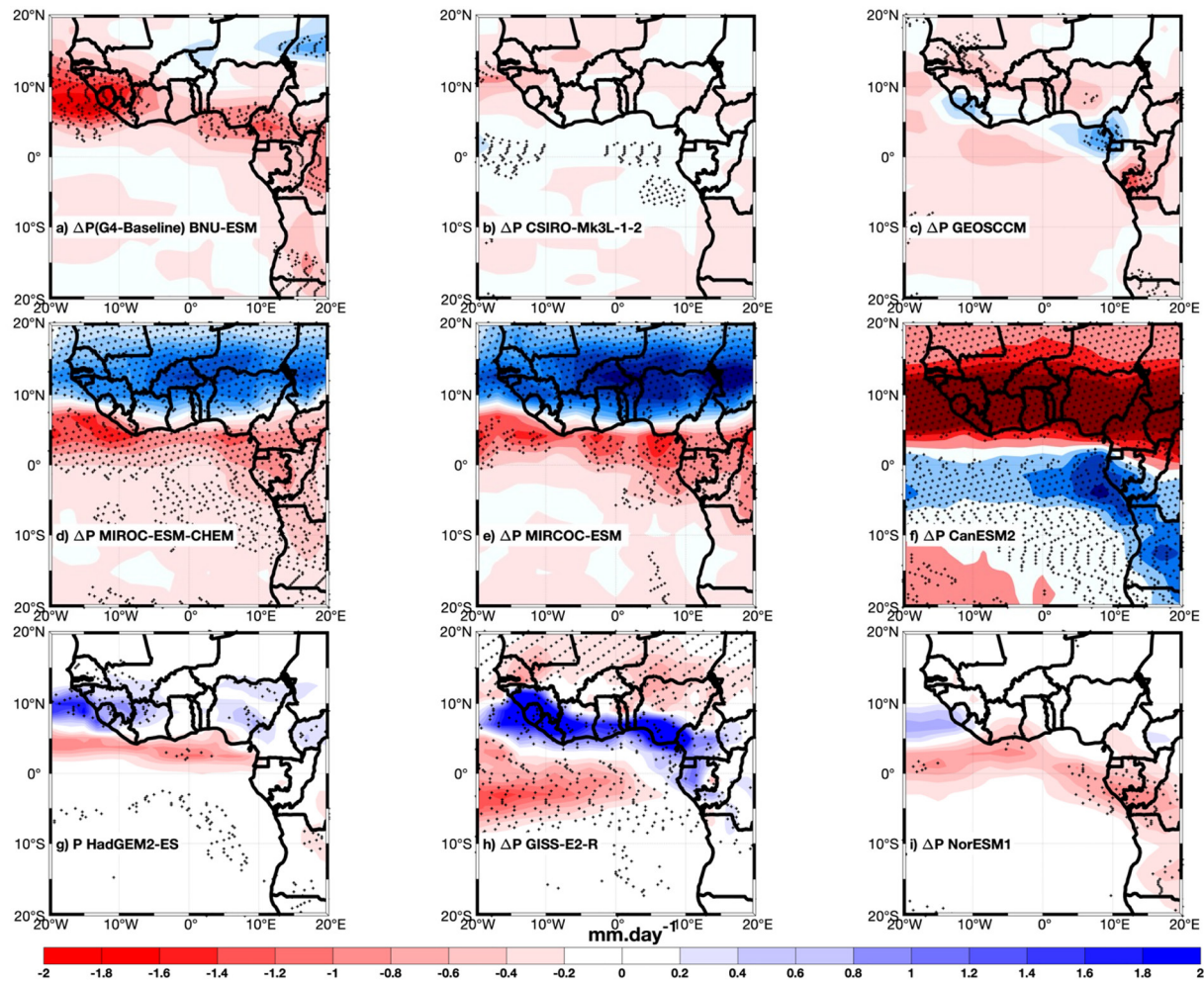


Figure 6. Precipitation changes between G4 and baseline simulations during monsoon period, July–October. The baseline or reference period is from 2010 to 2029 and the future period for G4 is from 2050 to 2069 for different models. The cross points represent the zone of significance at 95% confidence level.

different components of precipitation (Figures 7a and 7b). There is a negligible difference between the changes in P and the sum of the decomposition (Figure 7i), emphasizing that the decomposition method used is consistent in demonstrating changes in WASM. The ITCZ seasonally shifts north and south, in the Northern hemisphere summer and winter, as it moves toward the warmer hemisphere. In West Africa, the temperature contrast between the relatively warm land in the North and the relatively cool ocean in the South is greater under RCP4.5. This leads to northwards shift of the ITCZ over West Africa. Cheng et al. (2019) have demonstrated that during the boreal summer, the ITCZ position shifts to northward position under global warming conditions. When there are shifts in ITCZ position, the maxima precipitation zone is located farther north compared to its usual position. In conclusion, the dynamic process mainly drives the changes in precipitation under RCP4.5.

3.5. Impacts of Precipitation Changes and Its Main Causes Under G3

Under SAG, the spatial monthly distribution of P in the G3 simulation relative to that of the baseline shows the decrease in summer monsoon precipitation in West African regions (Figure 9a). This precipitation change is also significant in West African Countries (Figure 9a). As in the RCP4.5, the contribution of ΔP_{cross} to precipitation changes is also negligible under G3 simulations (Figure 9c). Under G3, ΔP_{therm} has a negligible contribution to the precipitation change due to the small changes in the surface-specific humidity relative to the baseline (Figures 8c and 9b). The dynamic terms (both the weak and shift terms) contribute to the precipitation change. The ΔP_{weak} component presents a similar pattern as that of precipitation change with a small contribution of ΔP_{shift} ($\sim 0.2 \text{ mm day}^{-1}$) of decrease (Figures 9a, 9c, and 9f). The contribution of ΔP_{shift} is associated with the

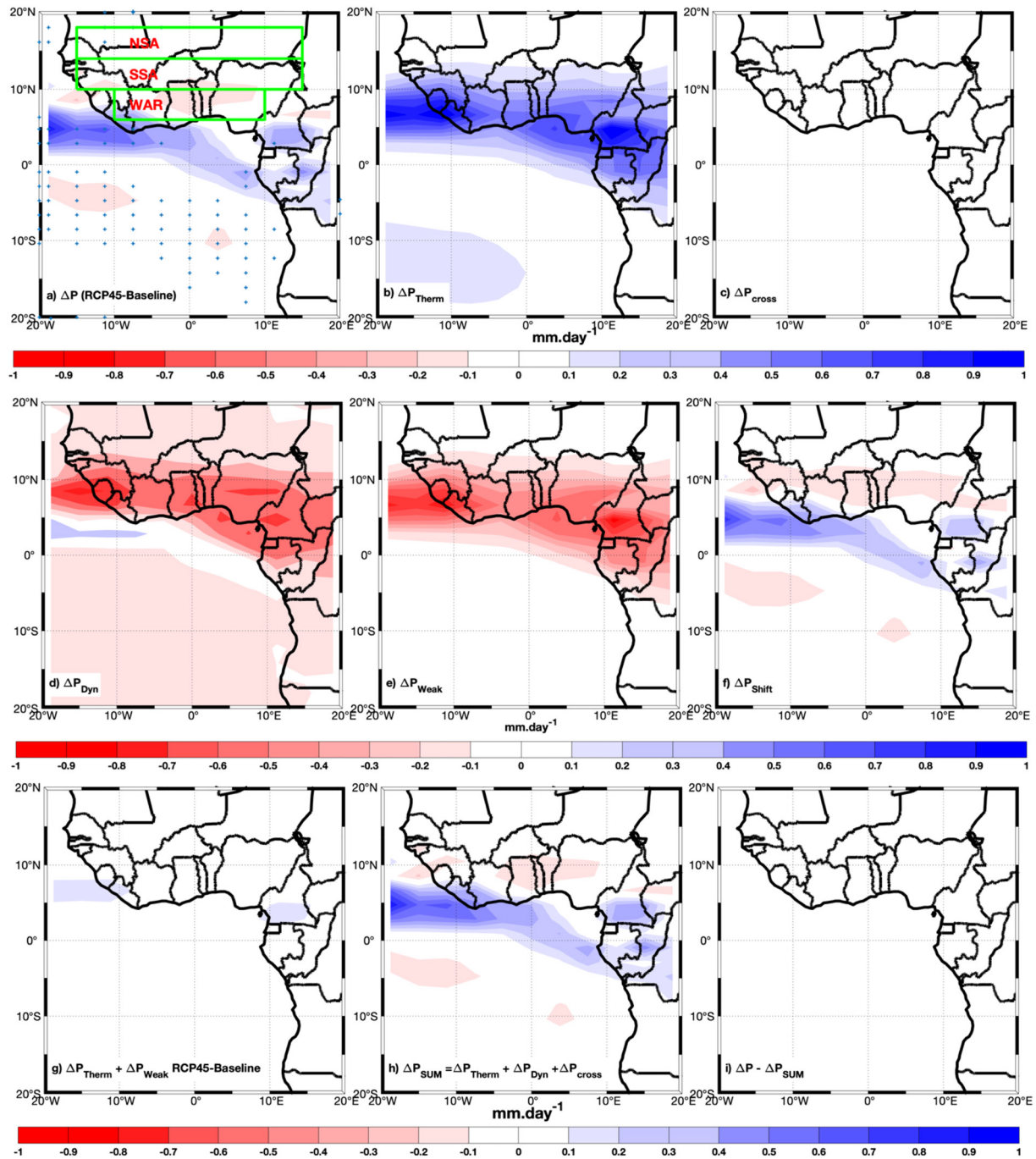


Figure 7. (a) Changes in monsoon precipitation under RCP4.5 related the baseline with its different terms, (b) thermodynamic (ΔP_{Therm}), (c) nonlinear cross term (ΔP_{cross}) and (d) dynamic (ΔP_{Dyn}). The dynamic component (ΔP_{Dyn}) is decomposed into (ΔP_{Weak}) and (ΔP_{Shift}); (g) presents the sum of $\Delta P_{Therm} + \Delta P_{Weak}$, (h) presents the sum of $\Delta P_{Therm} + \Delta P_{cross} + \Delta P_{Dyn}$, the difference between (a) (the model precipitation change) and (h) (the sum of all the components of precipitation change). NSA is Northern Sahel, SSA is Southern Sahel and WAR is the Western Africa Region.

low-level land-sea temperature contrast. Due to the seasonal variation in the solar radiation in the tropical region and the strong heat capacity of the ocean, the land would warm or cool faster than the ocean, and the low-level land-sea thermal contrast is strongly affected by solar radiation (Liu et al., 2019). Therefore, the use of SAG in the GeoMIP simulations could attenuate the amount of sunlight that reaches the Earth's surface; this process could contribute to reducing the low-level land-sea thermal contrast. This reduction of land-sea thermal contrast is responsible for the weakening of monsoon circulation and its shift. The change in monsoon precipitation under

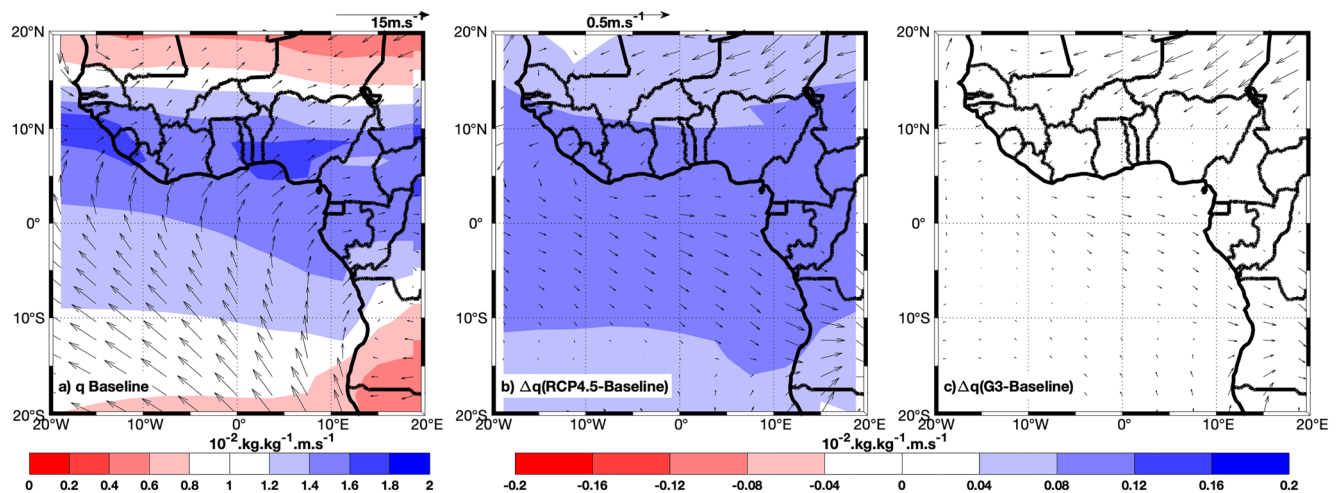


Figure 8. Spatial distributions of average monthly near surface specific humidity (in color) and surface wind field (vectors) at 955 hPa for the baseline simulation over 2010–2029, (b) differences (relative to the baseline) in mean surface specific humidity (color) and near-surface wind (vectors) under RCP4.5, 2050–2069 at same pressure level and (c) same as in (b) with G3 simulation.

G3 primarily based on the decomposition approach is similar to the sum of different components of precipitation decomposed (Figures 9a and 9h) and the difference between these two terms is negligible (Figure 9i). In conclusion, under G3, the change in precipitation is explained by the dynamical process, which leads to a weakened monsoon circulation and a shift in the monsoon precipitation distribution.

The precipitation changes and their various components are also presented in Figure 10 for three subregions, the NSA (18°N–14°N, 15°W–15°E), the SSA (14°N–10°N, 15°W–15°E), and the WAR (6°N–10°N, 10°W–10°E). Under RCP4.5, slight decreases of precipitation have been found (0.86% and 0.8%) in the NSA and SSA but these changes are not statistically significant (Figures 7a, 10a, and 10c) in both sub-regions contrary to the findings of Da-Allada et al. (2020) who reported a significant increase with RCP8.5 which is GLENS control simulation. The increase of precipitation (1.04%) has been obtained in Western Africa Region (WAR). This result suggests that under RCP4.5, the increase will be moderated in WAR. Under G3 simulation, during the summer period, significant precipitation decreases of 17.4% and 8.47% were observed in the NSA and SSA respectively. The deployment of SAG in these two regions can be effective at NSA and SSA. A decrease in precipitation (3.71%) was noted in WAR. In these three subregions, during the boreal summer, changes in precipitation relative to the baseline for RCP4.5 and G3 were important compared to those of evaporation (Figure 11) over SSA and WAR. The changes in rainfall exceed those of evaporation in SSA and WAR regions while the change in rainfall is similar to that of evaporation in NSA region. Under RCP4.5, the physical processes responsible for precipitation changes are associated with the shifts in monsoon circulation that influence monsoon precipitation (shift component in Figure 10). Although the thermodynamic change is positive in the same direction as the precipitation change. The weak component of dynamical precipitation change tends to cancel out the thermodynamic component (Figure 10). The thermodynamic contribution to precipitation change is considerably neglected due to opposite pattern of thermodynamic and weak components. Finally, the dynamic process becomes the dominant factor in precipitation changes outweighing the thermodynamic process. Under G3 simulation, changes in precipitation in the three regions followed a similar pattern to the weakened component of dynamic precipitation change (Figure 10).

4. Discussions

In this study, the historical precipitation of CMIP5 models have been validated by comparing these models with CMAP and GPCP observation. The precipitation changes under climate change and climate geo-engineering through the application of Stratospheric Aerosol Geoengineering have been determined over West Africa and Sahel region using RCP4.5 and G3/G4 models from GeoMIP simulations. These (G3/G4) simulations are two simulations of the stratospheric aerosol geoengineering experiments in GeoMIP Models. The possible impacts of SAG (G3/G4) and the RCP4.5 experiment on precipitations within the period of (2050–2069) have been

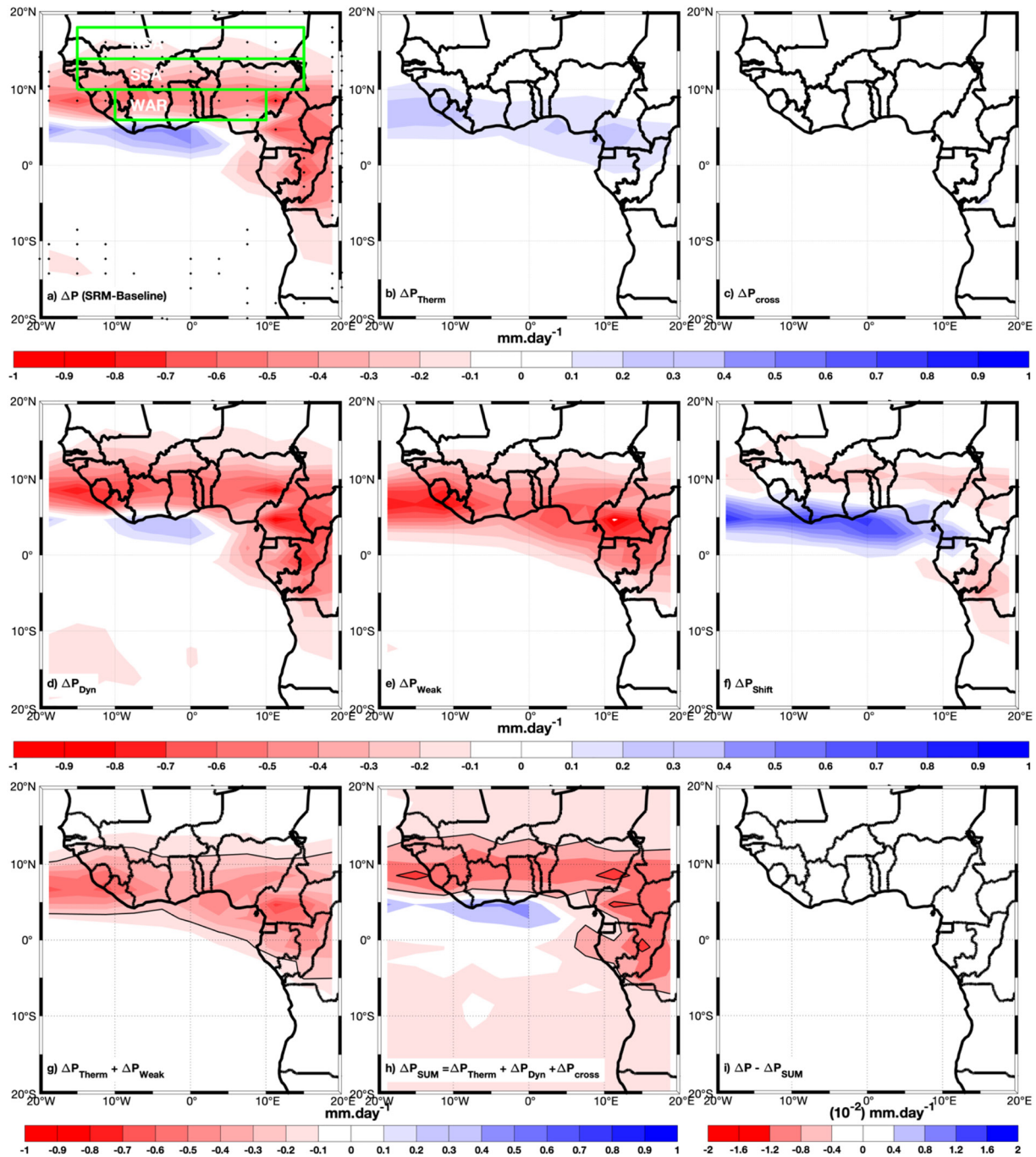


Figure 9. (a) Changes in monsoon precipitation under G3 related to the baseline with its different terms, (b) thermodynamic (ΔP_{Therm}), (c) nonlinear cross term (ΔP_{cross}) and (d) dynamic (ΔP_{dyn}). The dynamic component (ΔP_{dyn}) is decomposed into (ΔP_{weak}) and (ΔP_{shift}); (g) is the sum of $\Delta P_{\text{Therm}} + \Delta P_{\text{weak}}$, (h) presents the sum of $\Delta P_{\text{Therm}} + \Delta P_{\text{cross}} + \Delta P_{\text{dyn}}$, the difference between (a) (the model precipitation change) and (the sum of all the components of precipitation change) is (i). NSA is Northern Sahel, SSA is Southern Sahel and WAR is the Western Africa Region.

analyzed. The main mechanisms of rainfall changes have been determined using IPSL-CMA5-LR (due to availability of specific humidity data near 950 hPa) following the approach of Chadwick et al. (2013), which has been previously applied to investigate the mechanisms of rainfall changes over West Africa by Da-Allada et al. (2020).

The analysis of the ensemble precipitation changes suggests projected decreases in precipitation over West Africa (Tables S3 and S4 in Supporting Information S1) under G3 and G4 experiments while positive changes are mostly projected under global warming (Table S2 in Supporting Information S1). However, opposite

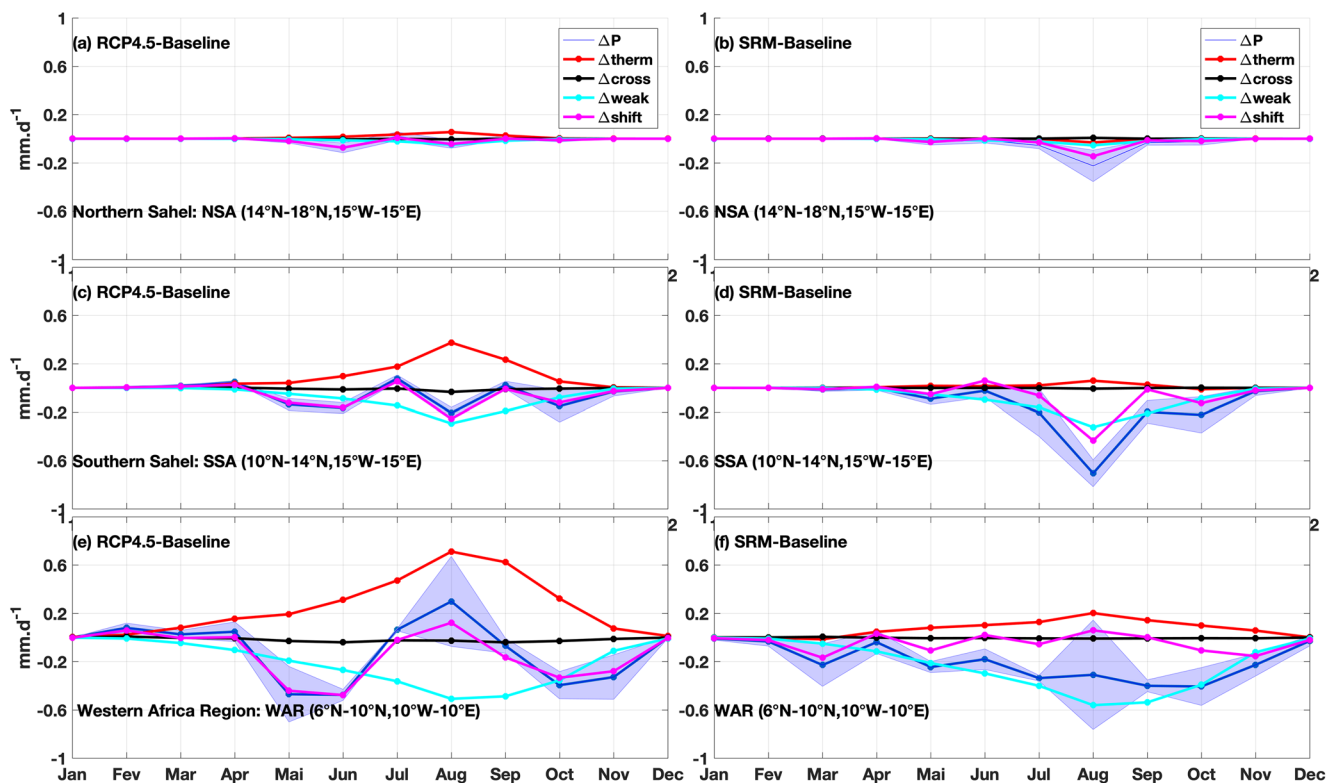


Figure 10. Seasonal cycles of precipitation changes and the different components of precipitation changes (see Figure 7) under RCP4.5 (left column) and G3 (IPSL-CM5A-LR) (right column) relative to the baseline for the Northern Sahel: NSA (a and b), Southern Sahel: SSA (c and d), and the Western Africa Region: WAR (e and f). Here the nonlinear component of precipitation. (ΔP_{cross}) is added and the blue shaded areas indicate the standard error on the precipitation change term. Changes in precipitation are obtained as in Figures 8 and 10. All units are mm day⁻¹.

changes are also projected by some of the models within the same experiments, for example, MIROC-ESM and MIROC-ESM-CHEM show an increase in precipitation under G4 experiments. The ensemble simulations present mostly the increase of rainfall under global warming although some decrease in precipitation has been obtained with some models. Some of these climate models can present overestimation or underestimation in precipitation. Dike et al. (2015) have pointed out the overestimation of precipitation biases in certain climate models over West Africa. They associated the reason with the fact that these models do not capture the changes in the Sea Surface Temperature within the Gulf of Guinea, which modulates the African monsoon circulation. These biases have revealed that the transition phase of African monsoon circulation is not well-represented by some models. However, most of these models simulate well the seasonal variability of precipitation in this region during the summer monsoon. The overestimation or underestimation of precipitation compared with the existing observation data can also be associated with some limitations on the configuration (forcing parameters) of climate models to well simulate the monsoon precipitation. These biases can also be attributed to the atmospheric component or the oceanic component set up of individual models, numerical schemes used by different groups of modeling, and physical parametrizations. Although, all of these models have been set up with a similar amount of SO₂ concentration injection from specific experiments, the way of sulfate aerosols is prescribed, and the location of initialization is also different from one modeling group to another. The numerical scheme of different theoretical equation resolution for each model is also different, the difference in spatial resolution of each model. We have presented some specifications patterns of each model in Table S1 of the Supporting Information S1. All those reasons can explain why opposite patterns can be obtained with these different models.

Most of the CMIP5 models are relatively in agreement with CMAP and GPCP precipitation. Their general patterns in estimating West African Monsoon precipitation during July and October are mostly comparable with that of observations rainfall. However, underestimation and overestimation of precipitation are also presented over some sub-areas of the West Africa from one model to another. CSIRO-Mk3L-1-2, BNU-ESM models present an underestimation of rainfall over the whole of West Africa and the Sahel Region while MPI-ESM models present a slight overestimation

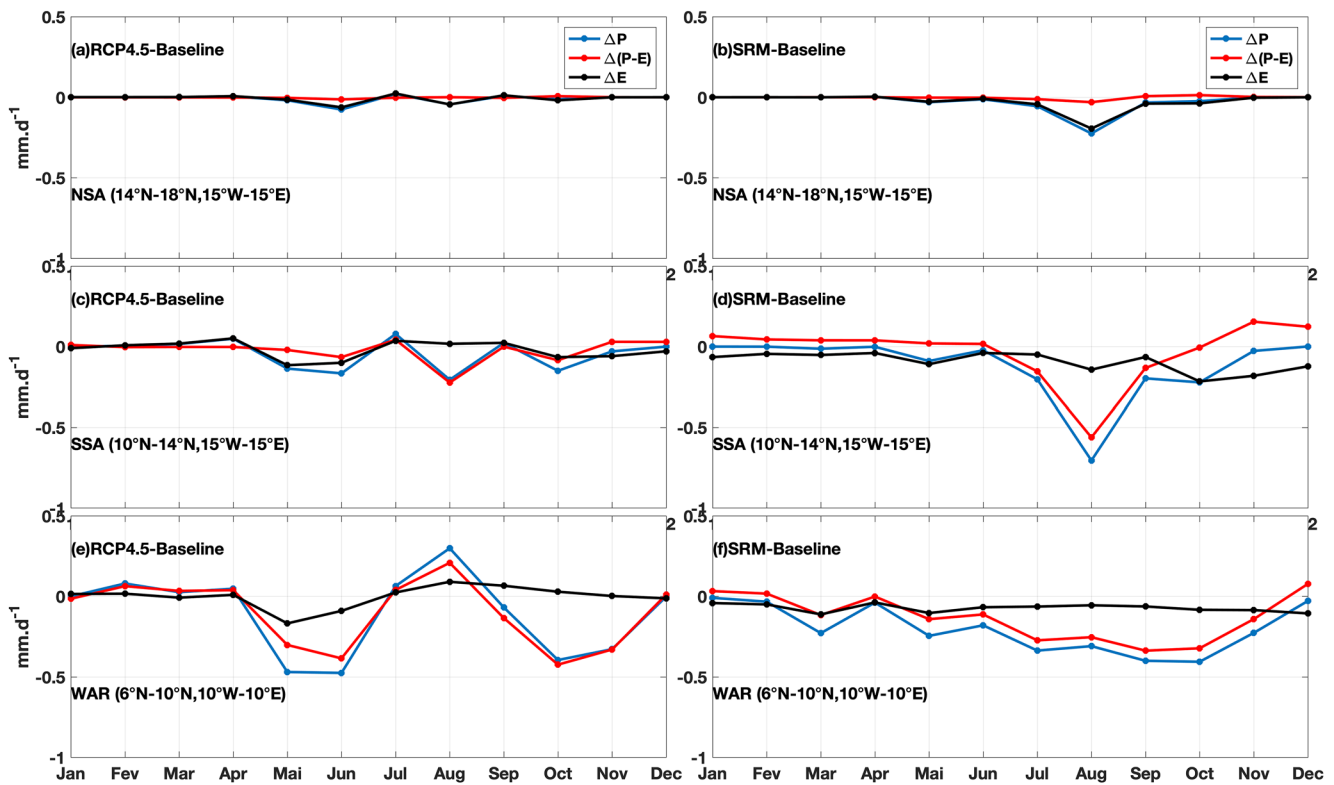


Figure 11. Monthly variability of precipitation, precipitation-evaporation and evaporation changes (relative to the present-day climate simulation) under RCP4.5 (left column) and G3 (right column) for the Northern of Sahel (a and b), Southern of Sahel (c and d), and the Western Africa region (e and f). Changes are for the period 2050–2069 relative to the present-day simulation. All units are mm day⁻¹.

of precipitation over these regions. Statistically, the historical ensemble of all the models present underestimation compared with CMAP observation. On the other hand, overestimation of precipitation has been also obtained over some coastal countries and the oceanic region adjacent to West Africa (Figures S1 and S2 in Supporting Information S1). Underestimation and overestimation in precipitation compared to observation are relatively reported by some of historical simulations. Recently Da-Allada et al. (2020) reported some underestimation of the historical GLENS simulation compared with CMAP and GPCP rainfall. These model biases over certain regions of West Africa and the Sahel region could be explained by the poor simulation of orographic forced ascent or the large uncertainty in the model precipitation estimates over this region (Akinsanola & Zhou, 2018; Da-Allada et al., 2020; Diallo et al., 2016).

In this study, we obtained a non-significant change in precipitation, which present a small negligible decrease under RCP4.5 with GeoMIP simulation (Figure 7a) with RCP4.5, which is a moderate scenario of global warming. This result is contrary to that of Da-Allada et al. (2020) who obtained an important decrease in rainfall using RCP8.5 simulations, with different background of GHGs. Under RCP4.5, slight decreases of precipitation have been found (-0.005 ± 0.075 i.e., 0.86%) and (-0.03 ± 0.17 i.e., 0.8%) in the NSA and SSA but these changes are not statistically significant (Figures 7a, 10a, and 10c) over both sub-regions contrary to those of Da-Allada et al. (2020) who found significant increase with RCP8.5 of GLENS control simulation. The increase of precipitation (0.09 ± 0.29 i.e., 1.04%) has been obtained in Western Africa Region (WAR). This result suggests that under RCP4.5, the increase will be moderated in WAR. The precipitation change is not also similar in NSA, while they have found a slight decrease in SSA under control simulation RCP8.5 during this same period. Positive and negative changes in precipitation have been obtained mainly with G4 simulations. The ensemble simulation shows the increase of precipitation although in some of these simulations the precipitation decreases. The contrary finding of this work in comparison with those of Da-Allada et al. (2020), the differences between model configurations and experimental conditions can explain this. It is also possible to fall on contrary results due to the configuration scheme of different models run by different institutions. This aspect allows us to understand that the possible impact of SAG on precipitation (increase or decrease of precipitation) can depend mainly on the data set, experiments, and model configuration (Land, atmosphere, and Ocean).

In this study, (IPSL-CM5A-LR, G3 experiment) has been used to assess the mechanisms responsible for the monsoon precipitation changes due to the accessibility of specific humidity at near-surface pressure level. In this study, only IPSL-CM5A-LR presents data of specific humidity spatial distribution near this pressure level at 955 hPa. All the rest of the models listed have a lower vertical resolution of specific humidity (q) at a different level. The near-surface level at which data are available for the rest of the model is 925 hPa of pressure, which is not able to explain the different mechanisms correctly according to the methods used in this paper. However, we applied the decomposition methods based on the available data of specific humidity in Supporting Information S1 for the ensemble simulations of G4 and G3 (Figures S4–S6 in Supporting Information S1). It is clearly shown for the pressure level lower than 955 hPa, the decomposition method is not able to well explain all the different changes through its components, as the difference between P and the sum of different components presents some biases. The results show that the dynamical processes are mostly responsible for the different changes, although thermodynamic processes can contribute to these changes.

This increase (decrease) of variation of thermodynamic term ΔP_{therm} is explained by the increase (decrease) of near surface specific humidity relative to the baseline (Figures 8a and 8b). While this component of precipitation increases, climatological precipitation is intensified. This term contributes to reinforcing or weakening the climatological precipitation pattern. ΔP_{cross} is the nonlinear cross term that takes into account the changes related to specific humidity and circulation. ΔP_{dyn} variation explains the change associated with the low-level monsoon winds, which are related to the sea-land thermal contrast (Li et al., 2019). Under global warming conditions, although ΔP_{therm} contribution cannot be neglected, ΔP_{dyn} is the major contributor responsible for the ΔP changes. The combination of the negative change of ΔP_{weak} (Figure 7e) tends to offset the positive change in ΔP_{therm} . The ΔP_{shift} component, which represents the monsoon circulation shift from the dynamic process, has similar patterns as ΔP . Under SAG conditions, although ΔP_{therm} change presents positive changes with this simulation, when we add the thermodynamical component to that of ΔP_{weak} , it appears that ΔP_{therm} is absorbed by ΔP_{weak} , showing again that thermodynamic contribution is not responsible for ΔP change. Under this scenario, ΔP change is mainly explained by the dynamical process and mostly by ΔP_{weak} , which presents negative change. Therefore, this change in rainfall is explained by weakening of monsoon circulation.

Using the same methodology as Cheng et al. (2019), the boreal summer efficacy of geoengineering that counterbalance the impacts of RCP4.5 (ratio of Geoengineering–RCP4.5 difference over RCP4.5–Baseline) for precipitation is calculated. The efficacy value >-1 leads to under compensation induced by geoengineering relative to baseline whereas the efficacy value <-1 suggests geoengineering leads to over compensation relative to baseline. In this work, we did not calculate the efficacy for NSA and SSA due to non-significant precipitation changes related to the baseline, which leads to negligible change of precipitation; therefore, we only focused our calculation in WAR under RCP4.5. We calculated the mean efficacy value of precipitation which is $-3.51 <-1$ (high over compensation) in WAR. Da-Allada et al. (2020) obtained -3.11 as a value of efficacy in WAR, based on this value they argue that the offset of warming in WAR region may need the use of 1/3 of RCP8.5 to limit their impact on precipitation. In this study, the value of the efficacy is -3.51 in WAR, more than three times (overcompensation), we then suggested in our study that the offset of warming can be done by around 1/3 of RCP4.5 amount to limit the dry biases on precipitation. The hydrological cycle in this region can be affected by the deployment of SAG. Thus, the application of SAG in the West African region using both G3 and CMIP5 simulations will overcompensate for the changes in precipitation in the Western African region. This recommends counterbalancing all warming would be going excessively far if the objective were to reestablish the Western Africa monsoon precipitation; rather, this would require restricting SAG arrangement to balancing 1/3 of RCP4.5 warming. As the connection between global mean warming and regional precipitation change is dependent upon enormous vulnerabilities, this model outcome ought to be taken into consideration in the monitoring of future climate.

5. Conclusion

This paper contributes to the analysis of monsoon precipitation changes and the mechanisms responsible for these changes during boreal summer in West Africa using CMIP5 and GeoMIP simulations. In general, all models reproduce relatively the monsoon precipitation patterns compared to observed data, and all models agree with the intensification of precipitation during WASM period. IPSL-CM5A-LR simulations have been used in this study to investigate the main mechanisms inducing precipitation changes under global warming and climate geoengineering. An increase in summer monsoon precipitation is slightly shown over the West Africa Region

and most accentuated over the coastal zone adjacent to West Africa countries located below 10°N under RCP4.5. These changes on monsoon P under RCP4.5 are mainly driven by the dynamic processes. Under G3 simulation, a decrease above 5°N during boreal summer has been reported in West Africa and Sahel region. This change in precipitation under G3 precipitation is mainly explained by the dynamic processes (both shift and weak terms), which leads to a weakened monsoon circulation and a shift in the distribution of monsoon precipitation. Three specific regions have been considered, NSA, the SSA, and the WAR. Under RCP4.5, during the monsoon period, non-significant precipitation decreases by $(0.005 \pm 0.075$ i.e., 0.86%) and $(0.03 \pm 0.17$ i.e., 0.8%) are reported in NSA and SSA respectively while an increase in precipitation $(0.09 \pm 0.29$ i.e., 1.04%) compared to present-day simulation in WAR region. However, with G3, relative to the baseline, the WASM rainfall, the precipitation decreases by $(0.10 \pm 0.12$ i.e., 17.4%) and $(0.36 \pm 0.29$ i.e., 8.47%), respectively in the NSA and SSA, respectively, while decreases $(0.34 \pm 0.25$ i.e., 3.71%) has been noted in WAR. Due to the non-significant precipitation changes over NSA and SSA, the efficacy mean has been considered only for WAR region. Using SAG will therefore have no major effect in the Sahel regions (NSA and SSA), whereas it can be highly effective in the WAR. The mean efficacy ratio of SAG (−3.51) determined during the monsoon period suggests a high over compensation in WAR. In this region, if the goal were to reestablish the Western African Monsoon precipitation, this work recommends that the organization of SAG should be restricted to balancing 1/3 of RCP4.5.

In agreement with previous studies (e.g., Cheng et al., 2019; Da-Allada et al., 2020), our results showed that WASM precipitation decrease also under G3 simulation as they recently found with GLENS simulations. This study is a contribution to the determination of the physical processes responsible for precipitation changes in the WAR using G3. Our findings indicated that changes in precipitation in this region are largely led by the changes in the monsoon circulation, which result from the reduction of the thermal gradient induced by the application of SAG. Understanding the mechanism of the precipitation decrease will contribute to improving and implementing the strategies for stratospheric aerosol injection to mitigate the effect of SAG on precipitation changes.

Conflict of Interest

The authors declare no conflicts of interest relevant to this study.

Data Availability Statement

The CMIP5 and GeoMIP simulations used in this study are available from the Earth System Grid Federation via this link <https://esgf-node.llnl.gov/>. More detail can be founded in Kravitz et al. (2011, 2013, 2019) and Tilmes et al. (2013a, 2013b), the citations details are in reference list. In-text data citation references are also provided for CMAP and GPCP, (Huffman et al., 1997; P. Xie & Arkin, 1997).

Acknowledgments

We acknowledge the financial support of the DEGREES Modelling Fund (DMF) of the DEGREES Initiative, which was established in 2010 by the Royal Society, Environmental Defense Fund and The World Academy of Sciences and is funded by the Open Philanthropy Project. All authors thank every group involved in CMIP5 model output data provided by the WHOI CMIP5 Community and we also thank the climate modeling group of the GeoMIP and the scientists managing the Earth System Grid data nodes who have assisted in making the GeoMIP output available. We acknowledge, Alan Robock, Ben Kravitz, Helene Muri, Andy Parker for GeoMIP data providing and their technical supports. We also acknowledge Kouakou Marcel for his help with this proof reading this paper. Special thanks for three anonymous reviewers for their relevant contribution in the different processes of the revisions of this work.

References

- Abiodun, B. J., Pal, J. S., Afiesimama, E. A., Gutowski, W. J., & Adedoyin, A. (2008). Simulation of West African monsoon using RegCM3 Part II: Impacts of deforestation and desertification. *Theoretical and Applied Climatology*, 93(3–4), 245–261. <https://doi.org/10.1007/s00704-007-0333-1>
- Akinsanola, A. A., & Zhou, W. (2018). Ensemble-based CMIP5 simulations of West African summer monsoon rainfall: Current climate and future changes. *Theoretical and Applied Climatology*, 136(3–4), 1021–1031. <https://doi.org/10.1007/s00704-018-2516-3>
- Bentsen, M., Bethke, I., Debernard, J. B., Iversen, T., Kirkevåg, A., Seland, Ø., et al. (2013). The Norwegian Earth system model, NorESM1-M—Part I: Description and basic evaluation of the physical climate. *Geoscientific Model Development*, 6(3), 687–720. <https://doi.org/10.5194/gmd-6-687-2013>
- Bürger, G., & Cubasch, U. (2015). The detectability of climate engineering. *Journal of Geophysical Research: Atmospheres*, 120(22), 11404–11418. <https://doi.org/10.1002/2015JD023954>
- Chadwick, R., Boutle, I., & Martin, G. (2013). Spatial patterns of precipitation change in CMIP5: Why the rich do not get richer in the tropics. *Journal of Climate*, 26(11), 3803–3822. <https://doi.org/10.1175/jcli-d-12-00543.1>
- Chadwick, R., Good, P., & Willett, K. (2016). A simple moisture advection model of specific humidity change over land in response to SST warming. *Journal of Climate*, 29(21), 7613–7632. <https://doi.org/10.1175/jcli-d-16-0241.1>
- Cheng, W., MacMartin, D. G., Dagon, K., Kravitz, B., Tilmes, S., Richter, J. H., et al. (2019). Soil moisture and other hydrological changes in a stratospheric aerosol geoengineering large ensemble. *Journal of Geophysical Research: Atmospheres*, 124(23), 12773–12793. <https://doi.org/10.1029/2018JD030237>
- Chou, C., & Neelin, J. (2004). Mechanisms of global warming impacts on regional tropical precipitation. *Journal of Climate*, 17(13), 2688–2701. [https://doi.org/10.1175/1520-0442\(2004\)017<2688:mogwio>2.0.co;2](https://doi.org/10.1175/1520-0442(2004)017<2688:mogwio>2.0.co;2)
- Chylek, P., Li, J., Dubey, M. K., Wang, M., & Lesins, G. (2011). Observed and model simulated 20th century Arctic temperature variability: Canadian Earth system model CanESM2. *Atmospheric Chemistry and Physics Discussions*, 11, 22893–22907. <https://doi.org/10.5194/acpd-11-22893-2011>

- Clarke, L. A., Taylor, M. A., Centella-Artola, A., Williams, M. S. M., Campbell, J. D., Bezanilla-Morlot, A., & Stephenson, T. S. (2021). The Caribbean and 1.5°C: Is SRM an option? *Atmosphere*, 12(3), 367. <https://doi.org/10.3390/atmos12030367>
- Collins, W. J., Bellouin, N., Doutriaux-Boucher, M., Gedney, N., Halloran, P., Hinton, T., et al. (2011). Development and evaluation of an Earth-System model—HadGEM2. *Geoscientific Model Development*, 4(2), 997–1062.
- Crutzen, P. J. (2006). Albedo enhancement by stratospheric sulfur injections: A contribution to resolve a policy dilemma? *Climatic Change*, 77(3), 211. <https://doi.org/10.1007/s10584-006-9101-y>
- Da-Allada, C. Y., Baloitcha, E., Alamou, E. A., Awo, F. M., Bonou, F., Pomalegni, Y., et al. (2020). Changes in West African summer monsoon precipitation under stratospheric aerosol geoengineering. *Earth's Future*, 8(7), e2020EF001595. <https://doi.org/10.1029/2020EF001595>
- Diallo, I., Giorgi, F., Tall, M., Mariotti, L., & Gaye, A. T. (2016). Projected changes of summer monsoon extreme and hydroclimatic regimes over West Africa for the twenty-first century. *Climate Dynamics*, 47(12), 3931–3954. <https://doi.org/10.1007/s00382-016-3,052-4>
- Dike, V., Shimizu, M., Diallo, M., Lin, Z., Nwofor, O., & Chineke, T. (2015). Modelling present and future African climate using CMIP5 scenarios in HadGEM2-ES. *International Journal of Climatology*, 35(1), 1784–1799. <https://doi.org/10.1002/joc.4084>
- Dong, B., & Sutton, R. (2015). Dominant role of greenhouse-gas forcing in the recovery of Sahel rainfall. *Nature Climate Change*, 5(8), 757–760. <https://doi.org/10.1038/nclimate2664>
- Dufresne, J.-L., Foujols, M.-A., Denvil, S., Caubel, A., Marti, O., Aumont, O., et al. (2013). Climate change projections using the IPSL-CM5 Earth system model: From CMIP3 to CMIP5. *Climate Dynamics*, 40(9), 2123–2165. <https://doi.org/10.1007/s00382-012-1636-1>
- Duncan, B. N., Strahan, S. E., Yoshida, Y., Steenrod, S. D., & Livesey, N. (2007). Model study of the cross-tropopause transport of biomass burning pollution. *Atmospheric Chemistry and Physics*, 7(14), 3713–3736. <https://doi.org/10.5194/acp-7-3713-2007>
- Froidurot, S., & Diedhiou, A. (2017). Characteristics of wet and dry spells in the West African monsoon system. *Atmospheric Science Letters*, 18(3), 125–131. <https://doi.org/10.1002/asl.734>
- Govindasamy, B., & Caldeira, K. (2000). Geoengineering Earth's radiation balance to mitigate CO₂-induced climate change. *Geophysical Research Letters*, 27(14), 2141–2144. <https://doi.org/10.1029/1999gl006086>
- Haywood, J. M., Jones, A., Bellouin, N., & Stephenson, D. (2013). Asymmetric forcing from stratospheric aerosols impacts Sahelian rainfall. *Nature Climate Change*, 3(7), 660–665. <https://doi.org/10.1038/nclimate1857>
- Heckendorn, P., Weisenstein, D., Fueglistaler, S., Luo, B. P., Rozanov, E., Schraner, M., et al. (2009). The impact of geoengineering aerosols on stratospheric temperature and ozone. *Environmental Research Letters*, 4(4), 045108. <https://doi.org/10.1088/1748-9326/4/4/045108>
- Held, I. M., & Soden, B. J. (2006). Robust responses of the hydrological cycle to global warming. *Journal of Climate*, 19(21), 5686–5699. <https://doi.org/10.1175/jcli3990.1>
- Huffman, G. J., Adler, R. F., Arkin, P., Chang, A., Ferraro, R., Gruber, A., et al. (1997). The global precipitation Climatology project (GPCP) combined precipitation dataset [Dataset]. Bulletin of the American Meteorological Society, 78(1), 5–20. [https://doi.org/10.1175/1520-0477\(1997\)078<0005:TGPCPG>2.0.CO;2](https://doi.org/10.1175/1520-0477(1997)078<0005:TGPCPG>2.0.CO;2)
- Janicot, S. (1992). Spatiotemporal variability of West African rainfall. Part I: Regionalizations and typings. *Journal of Climate*, 5(5), 489–497. [https://doi.org/10.1175/1520-0442\(1992\)005<0489:svowar>2.0.co;2](https://doi.org/10.1175/1520-0442(1992)005<0489:svowar>2.0.co;2)
- Kent, C., Chadwick, R., & Rowell, D. P. (2015). Understanding uncertainties in future projections of seasonal tropical precipitation. *Journal of Climate*, 28(11), 4390–4413. <https://doi.org/10.1175/jcli-d-14-00613.1>
- Kravitz, B., Caldeira, K., Boucher, O., Robock, A., Rasch, P. J., Alterskjær, K., et al. (2013). Climate model response from the geoengineering model intercomparison project (GeoMIP) [Dataset]. *Journal of Geophysical Research: Atmospheres*, 118(15), 8320–8332. <https://doi.org/10.1002/jgrd.50646>
- Kravitz, B., MacMartin, D. G., Tilmes, S., Richter, J. H., Mills, M. J., Cheng, W., et al. (2019). Comparing surface and stratospheric impacts of geoengineering with different SO₂ injection strategies [Dataset]. *Journal of Geophysical Research: Atmospheres*, 124(14), 7900–7918. <https://doi.org/10.1029/2019JD030329>
- Kravitz, B., Robock, A., Boucher, O., Schmidt, H., Taylor, K. E., Stenchikov, G., & Schulz, M. (2011). The geoengineering model intercomparison project (GeoMIP) [Dataset]. *Atmospheric Science Letters*, 12(2), 162–167. <https://doi.org/10.1002/asl.316>
- Lamb, P. J. (1982). Persistence of Sahelian drought/nature. Retrieved from <https://www.nature.com/articles/299046a0>
- Lazenby, M. J., Todd, M. C., Chadwick, R., & Wang, Y. (2018). Future precipitation projections over central and southern Africa and the adjacent Indian Ocean: What causes the changes and the uncertainty? *Journal of Climate*, 31(12), 4807–4826. <https://doi.org/10.1175/JCLI-D-17-0311.1>
- Lélé, M. I., Leslie, L. M., & Lamb, P. J. (2015). Analysis of low-level atmospheric moisture transport associated with the West African Monsoon. *Journal of Climate*, 28(11), 4414–4430. <https://doi.org/10.1175/jcli-d-14-00746.1>
- Lenton, T. M., & Vaughan, N. E. (2009). Interactive comment on “The radiative forcing potential of different climate geoengineering options” by T. M. Lenton and N. E. Vaughan. Discussion Paper, 15.
- Li, Z., Sun, Y., Li, T., Ding, Y., & Hu, T. (2019). Future changes in East Asian summer monsoon circulation and precipitation under 1.5 to 5°C of warming. *Earth's Future*, 7(12), 1391–1406. <https://doi.org/10.1029/2019EF001276>
- Liu, Y., Cai, W., Sun, C., Song, H., Cobb, K. M., Li, J., et al. (2019). Anthropogenic aerosols cause recent pronounced weakening of Asian Summer Monsoon relative to last four centuries. *Geophysical Research Letters*, 46(10), 5469–5479. <https://doi.org/10.1029/2019GL082497>
- MacMartin, D. G., Wang, W., Kravitz, B., Tilmes, S., Richter, J. H., & Mills, M. J. (2019). Timescale for detecting the climate response to stratospheric aerosol geoengineering. *Journal of Geophysical Research: Atmospheres*, 124(3), 1233–1247. <https://doi.org/10.1029/2018JD028906>
- Mera, R., Laing, A. G., & Semazzi, F. (2014). Moisture variability and multiscale interactions during spring in West Africa. *Monthly Weather Review*, 142(9), 3178–3198. <https://doi.org/10.1175/mwr-d-13-00175.1>
- Monerie, P., Robson, J., Dong, B., Hodson, D. L. R., & Klingaman, N. P. (2019). Effect of the Atlantic multidecadal variability on the global monsoon. *Geophysical Research Letters*, 46(3), 1765–1775. <https://doi.org/10.1029/2018GL080903>
- Nicholson, S. E. (2013). The West African Sahel: A review of recent studies on the rainfall regime and its interannual variability. *ISRN Meteorology*, 1–32. <https://doi.org/10.1155/2013/453521>
- Nicholson, S. E., & Grist, J. P. (2003). The seasonal evolution of the atmospheric circulation over West Africa and equatorial Africa. *Journal of Climate*, 16(7), 1013–1030. [https://doi.org/10.1175/1520-0442\(2003\)016<1013:tseota>2.0.co;2](https://doi.org/10.1175/1520-0442(2003)016<1013:tseota>2.0.co;2)
- Odoulami, R. C., New, M., Wolski, P., Guillemet, G., Pinto, I., Lennard, C., et al. (2020). “Stratospheric aerosol geoengineering could lower future risk of ‘Day Zero’ level droughts in Cape Town”. *Environmental Research Letters*, 15(12), 124007. <https://doi.org/10.1088/1748-9326/abbf13>
- Okoro, U. K., Chen, W., & Nath, D. (2018). Recent variations in geopotential height associated with West African monsoon variability. *Meteorology and Atmospheric Physics*, 131(3), 553–565. <https://doi.org/10.1007/s00703-018-0593-6>
- Parth Sarthi, P., Kumar, P., & Ghosh, S. (2016). Possible future rainfall over Gangetic Plains (GP), India, in multi-model simulations of CMIP3 and CMIP5. *Theoretical and Applied Climatology*, 124(3), 691–701. <https://doi.org/10.1007/s00704-015-1447-5>

- Pinto, I., Jack, C., Lennard, C., Tilmes, S., & Odoulami, R. C. (2020). Africa's climate response to solar radiation management with stratospheric aerosol. *Geophysical Research Letters*, 47(2), e2019GL086047. <https://doi.org/10.1029/2019GL086047>
- Pomposi, C., Kushnir, Y., & Giannini, A. (2015). Moisture budget analysis of SST-driven decadal Sahel precipitation variability in the twentieth century. *Climate Dynamics*, 44(11), 3303–3321. <https://doi.org/10.1007/s00382-014-2382-3>
- Redelsperger, J.-L., Thorncroft, C. D., Diedhiou, A., Lebel, T., Parker, D. J., & Polcher, J. (2006). African monsoon multidisciplinary analysis: An international research project and field campaign. *Bulletin of the American Meteorological Society*, 87(12), 1739–1746. <https://doi.org/10.1175/BAMS-87-12-1739>
- Robock, A., Marquardt, A., Kravitz, B., & Stenchikov, G. (2009). Benefits, risks, and costs of stratospheric geoengineering. *Geophysical Research Letters*, 36(19), L19703. <https://doi.org/10.1029/2009GL039209>
- Roehrig, R., Bouniol, D., Guichard, F., Hourdin, F., & Redelsperger, J.-L. (2013). The present and future of the West African monsoon: A process-oriented assessment of CMIP5 simulations along the AMMA transect. *Journal of Climate*, 26(17), 6471–6505. <https://doi.org/10.1175/JCLI-D-12-00505.1>
- Sanogo, S., Fink, A. H., Omotosho, J. A., Ba, A., Redl, R., & Ermert, V. (2015). Spatio-temporal characteristics of the recent rainfall recovery in West Africa. *International Journal of Climatology*, 35(15), 4589–4605. <https://doi.org/10.1002/joc.4309>
- Schmidt, G. A., Kelley, M., Nazarenko, L., Ruedy, R., Russell, G. L., Aleinov, I., et al. (2014). Configuration and assessment of the GISS ModelE2 contributions to the CMIP5 archive. *Journal of Advances in Modeling Earth Systems*, 6(1), 141–184. <https://doi.org/10.1002/2013MS000265>
- Schneider, T., Bischoff, T., & Haug, G. H. (2014). Migrations and dynamics of the intertropical convergence zone. *Nature*, 513(7516), 45–53. <https://doi.org/10.1038/nature13636>
- Sheffield, J., Barrett, A. P., Colle, B., Nelun Fernando, D., Fu, R., Geil, K. L., et al. (2013). North American climate in CMIP5 experiments. Part I: Evaluation of historical simulations of continental and regional Climatology. *Journal of Climate*, 26(23), 9209–9245. <https://doi.org/10.1175/JCLI-D-12-00592.1>
- Tilmes, S., Fasullo, J., Lamarque, J.-F., Marsh, D. R., Mills, M., Alterskjaer, K., et al. (2013a). The hydrological impact of geoengineering in the geoengineering model intercomparison project (GeoMIP) [Dataset]. *Journal of Geophysical Research: Atmospheres*, 118(19), 11–036. <https://doi.org/10.1002/jgrd.50868>
- Tilmes, S., Fasullo, J., Lamarque, J.-F., Marsh, D. R., Mills, M., Alterskjaer, K., et al. (2013b). The hydrological impact of geoengineering in the geoengineering model intercomparison project (GeoMIP). *Journal of Geophysical Research: Atmospheres*, 118(19), 11036–11058. <https://doi.org/10.1002/jgrd.50868>
- Tilmes, S., Garcia, R. R., Kinnison, D. E., Gettelman, A., & Rasch, P. J. (2009). Impact of geoengineered aerosols on the troposphere and stratosphere. *Journal of Geophysical Research*, 114(D12), D12305. <https://doi.org/10.1029/2008JD011420>
- Vertenstein, M., Craig, T., Middleton, A., Feddema, D., & Fischer, C. (2010). CCSM4.0 User's Guide. Retrieved from http://www.cesm.ucar.edu/models/ccsm4.0/ccsm_doc/ug.pdf
- Watanabe, S., Hajima, T., Sudo, K., Nagashima, T., Takemura, T., Okajima, H., et al. (2011). MIROC-ESM 2010: Model description and basic results of CMIP5-20c3m experiments. *Geoscientific Model Development*, 4(4), 845–872. <https://doi.org/10.5194/gmd-4-845-2011>
- Weller, E., Jakob, C., & Reeder, M. J. (2019). Understanding the dynamic contribution to future changes in tropical precipitation from low-level convergence lines. *Geophysical Research Letters*, 46(4), 2196–2203. <https://doi.org/10.1029/2018GL080813>
- Xie, P., & Arkin, P. A. (1997). Global precipitation: A 17-year monthly analysis based on gauge observations, satellite estimates, and numerical model outputs. *Bulletin of the American Meteorological Society*, 78(11), 2539–2558. [https://doi.org/10.1175/1520-0477\(1997\)078<2539:gpayma>2.0.co;2](https://doi.org/10.1175/1520-0477(1997)078<2539:gpayma>2.0.co;2)
- Xue, Y., & Shukla, J. (1993). The influence of land surface properties on Sahel climate. Part 1: Desertification. *Journal of Climate*, 6(12), 2232–2245. [https://doi.org/10.1175/1520-0442\(1993\)006<2232:tiolsp>2.0.co;2](https://doi.org/10.1175/1520-0442(1993)006<2232:tiolsp>2.0.co;2)